

# Charge-fluctuation contribution to the Raman response in superconducting cuprates

S. Caprara, C. Di Castro, M. Grilli, and D. Suppa

<sup>1</sup>*Istituto Nazionale di Fisica della Materia, Unità Roma 1 and SMC Center, and Dipartimento di Fisica  
Università di Roma "La Sapienza" piazzale Aldo Moro 5, I-00185 Roma, Italy*

(Dated: June 25, 2018)

We calculate the Raman response contribution due to collective modes, finding a strong dependence on the photon polarizations and on the characteristic wavevectors of the modes. We compare our results with recent Raman spectroscopy experiments in underdoped cuprates,  $\text{La}_{2-x}\text{Sr}_x\text{CuO}_4$  and  $(\text{Y}_{1.97}\text{Ca}_{0.3})\text{Ba}_2\text{CuO}_{6.05}$ , where anomalous low-energy peaks are observed, which soften upon lowering the temperature. We show that the specific dependence on doping and on photon polarizations of these peaks is only compatible with charge collective excitations at finite wavelength.

PACS numbers: 74.20.Mn, 78.30.-j, 74.72.-h, 71.45.Lr

There is an increasing experimental evidence that in the high  $T_c$  superconducting cuprates there are finite-energy excitations, which are distinct from the usual single-particle excitations characterizing the spectra of standard metals. In optical conductivity there are many examples of absorption peaks at finite frequencies, which are quite distinct from the zero-energy Drude peak, occurring in hole-doped [ $\text{La}_{2-x}\text{Sr}_x\text{CuO}_4$  (LSCO) [1],  $\text{La}_{1.6-x}\text{Nd}_{0.4}\text{Sr}_x\text{CuO}_4$  (LNSCO) [2],  $\text{Bi}_2\text{Sr}_2\text{CuO}_6$  (Bi2201) [3]] as well as in electron-doped materials [ $\text{Nd}_{2-x}\text{Ce}_x\text{CuO}_4$  (NCCO) [4]]. In all these cases absorption peaks are observed below  $200 \text{ cm}^{-1}$  which substantially soften upon decreasing the temperature  $T$ . It is natural to assign to these excitations a collective character. Moreover in the case of Bi2201 there is a clear evidence of scaling properties for the finite-frequency absorption [5]. This suggests that these excitations are nearly critical fluctuations associated to some criticality occurring in the cuprates below a critical line  $T^*(x)$ , ending near optimal doping at  $T = 0$ . The proposal of a quantum critical point in the strongly underdoped [6] or near optimal doping [7, 8, 9, 10, 11] is by now acquiring consensus in the community, but the nature of the ordered phase still remains debated. In this regard it is quite important to establish whether the collective modes (CM) responsible for the finite-frequency absorptions occur at finite wavevectors and are therefore associated to some form of spin and/or charge spatial ordering [6, 8] or have infinite wavelength [7, 9].

In order to clarify this issue, in this letter we calculate the Raman response contribution due to collective charge-order (CO) excitations associated to stripe fluctuations and eventually use our results to interpret recent findings of Raman-scattering experiments [12, 13]. Raman scattering is an important tool in the above issue for several reasons. First of all it is a probe directly accessing the bulk properties in the relevant frequency range. Most importantly, a suitable choice of the polarization of the incoming and outgoing photons selects the regions in momentum space from where excitations are originated [14]. As a consequence, characteristic features arise in

the Raman response with distinct doping and polarization dependencies [12, 13], which in turn allow to extract valuable informations about the momentum dependence of the excitations. This is the main issue of this work. We consider the doping-dependent line  $T_{CO}(x) \sim T^*(x)$  [15]. In the underdoped regime below this line the system would order in the absence of competing effects. Therefore strong CO fluctuations are present in a large portion of the phase diagram and provide an *additional* channel for the Raman response, besides the usual one obtained from Fermi-liquid quasiparticles (QP). The role of fluctuations in the response functions was established by Aslamazov and Larkin for the paraconductivity in superconductors [16]. This theory was extended to the particle-hole channel for one-dimensional charge-density-wave systems in Refs.17, 18. In this latter case a partial cancellation leads to a less singular paraconductivity as compared to the particle-particle case. Here we reconsider this scheme in two dimensions for the Raman response diagrammatically represented in Figs. 1(a) and 1(b) involving the incommensurate charge CM. We find that the above cancellation does not generically occur for the corresponding Raman diagrams, generating important contributions, which in turn depend on the selected symmetry. We will argue that only these contributions account for the *strong* symmetry dependence of the Raman response. Other diagrams with self-energy and vertex corrections are weakly anisotropic and provide the usual weakly temperature-dependent QP contribution. Specifically each dashed line appearing in the Raman response in Fig. 1 (a,b) is the gaussian diffusive CM propagator in Matsubara frequencies

$$D(\mathbf{q}, \omega_m) = (|\omega_m| + \Omega_{\mathbf{q}})^{-1}, \quad (1)$$

where  $\Omega_{\mathbf{q}} = \nu|\mathbf{q} - \mathbf{q}_c|^2 + m(x, T)$  with  $\nu$  a constant electronic energy scale (we consider a unit lattice spacing).  $m(x, T)$  is the mass of the CM and encodes the distance from the critical line  $T_{CO}(x)$ . This propagator is dominant at zero frequency and  $\mathbf{q} = \mathbf{q}_c$ , the wavevector setting the modulation of the most singular charge fluctua-

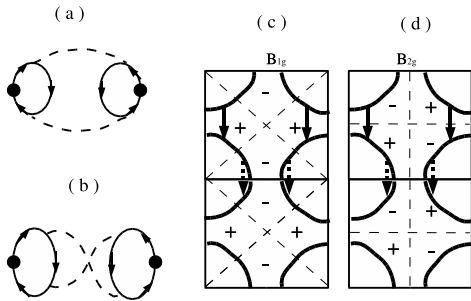


FIG. 1: Direct (a) and crossed (b) diagrams for the fluctuation contributions to Raman spectra. The dots represent Raman vertices. Solid lines represent fermionic QP propagators and dashed lines represent CM propagators. (c) and (d): Hot spots joined by the critical wavevector  $\mathbf{q}_c = (0, -q_c)$  represented by arrows. Equivalent hot spots have arrows of the same type (solid or dashed). The + (-) sign mark the regions where the  $B_{1g}$  and  $B_{2g}$  vertices are positive (negative).

tions. The fermionic loop in Fig. 1(a,b) has the form

$$\Lambda_{\alpha,\beta}(\Omega_l; \mathbf{q}, \omega_m) = CT \sum_n \sum_k \gamma_{\alpha,\beta}(\mathbf{k}) G(\mathbf{k}, \varepsilon_n + \Omega_l) \times G(\mathbf{k} - \mathbf{q}, \varepsilon_n - \omega_m) G(\mathbf{k}, \varepsilon_n), \quad (2)$$

where  $\gamma_{\alpha,\beta}(\mathbf{k}) \equiv \partial^2 E_{\mathbf{k}} / \partial k_{\alpha} \partial k_{\beta}$  and  $C$  is a constant determined by the coupling of the Raman vertex with the incoming and outgoing photons and the coupling  $g$  of the CM with the fermions. The choice of the  $\alpha$  and  $\beta$  components depends on the polarization of the incoming and outgoing photons [14]. A suitable choice of these polarizations corresponds to specific projections of the  $\gamma(\mathbf{k})$  vertex on cubic harmonics of the square lattice. To start our discussion we chose the polarization corresponding to a Raman vertex with  $B_{1g}$  symmetry  $\gamma_{B_{1g}} = \cos k_x - \cos k_y$  vanishing along the  $(0,0) \rightarrow (\pm\pi, \pm\pi)$  directions. We are interested in the dominant contributions of the diagrams in Fig. 1(a,b), which occur when the CM are around  $\mathbf{q}_c$ . Therefore we set  $\mathbf{q} = \mathbf{q}_c$  in Eq. (2). In the  $k$  summation the largest contribution is obtained when the three fermions are around the so-called hot spots, that is those regions on the Fermi surface which can be connected by  $\mathbf{q}_c$ . For each given  $\mathbf{q}_c$  in Eq. (2), to avoid cancellations, the sum over  $k$  must encounter equivalent hot spots where the vertex  $\gamma_{B_{1g}}(k)$  does not change sign. Since  $\gamma_{B_{1g}}$  changes sign under the  $\pm x$  vs.  $\pm y$  interchange, this condition is fulfilled by stripes or eggbox CO fluctuations at not too small doping [8, 19, 20, 21], where  $\mathbf{q}_c \approx 2\pi(\pm 0.2, 0), 2\pi(0, \pm 0.2)$  [see Fig. 1(c)]. On the other hand, when for the same  $\mathbf{q}_c$  the  $B_{2g}$  vertex  $\gamma_{B_{2g}} = \sin k_x \sin k_y$  is considered in Eq. (2), the leading contribution from hot spots vanishes since the equivalent “available” hot spots [see Fig. 1(d)] give contributions from regions where  $\gamma_{B_{2g}}$  is opposite in sign. With similar arguments one can show both in the superconducting [22] and in the normal phase, that spin CM at  $\mathbf{q}_c = (\pm\pi, \pm\pi)$ , although having the similar hot spots as the CO ones, give rise to non-vanishing

vertices for the  $A_{1g}$  symmetry only. The same holds for spin CM with diagonal incommensurate wavevectors  $\mathbf{q}_c \approx (\pm(\pi - \delta), \pm(\pi - \delta))$ , which is the case of LSCO at low doping ( $x \leq 0.04$ ) [23]. On the other hand, at higher doping, for small vertical and horizontal incommensuration  $\mathbf{q}_c = (\pm(\pi - \delta), \pm\pi), (\pm\pi, \pm(\pi - \delta))$ , there is no complete cancellation in the  $B_{1g}$  symmetry. This small contribution could add to the CO contribution that we are going to evaluate from the diagrams of Fig. 1(a,b), but cannot explain the anomalous Raman response in the deeply underdoped regime.

The resulting CM contribution to  $B = B_{1g}, B_{2g}$  Raman scattering is given by

$$\Delta\chi''_B = \Lambda_B^2 \int_0^{\infty} dz [b(z - \omega/2) - b(z + \omega/2)] \times \frac{z_+ z_-}{z_+^2 - z_-^2} [F(z_-) - F(z_+)] \quad (3)$$

where  $b(z)$  is the Bose function,

$$F(z) \equiv \frac{1}{z} \left[ \arctan\left(\frac{\omega_0}{z}\right) - \arctan\left(\frac{m}{z}\right) \right], \quad (4)$$

and  $z_{\pm} \equiv (z \pm \omega/2)(1 + (z \pm \omega/2)^2/\omega_0^2)$ . Here  $\omega_0 \sim 100 - 500 \text{ cm}^{-1}$  is an ultraviolet cutoff of the order of the frequency of the phonons most strongly coupled to the electrons and driving the systems near the CO instability [15]. The above expression of  $\Delta\chi''$  is actually calculated by considering CO collective modes with a semiphenomenological spectral density of the form

$$A(\omega, \Omega_{\mathbf{q}}) = \frac{\omega \left[ 1 + \left( \frac{\omega}{\omega_0} \right)^2 \right]}{\omega^2 \left[ 1 + \left( \frac{\omega}{\omega_0} \right)^2 \right]^2 + \Omega_{\mathbf{q}}^2} \quad (5)$$

In the limit of infinite  $\omega_0$ , one recovers the spectral density of the above critical diffusive propagator  $D(\mathbf{q}, \omega_m)$ .

Experimentally [12] in  $\text{La}_{1.9}\text{Sr}_{0.1}\text{CuO}_4$  an anomalous Raman absorption is observed in the  $B_{1g}$  symmetry, while the behavior of the  $B_{2g}$  spectra can be accounted for by QP only. Moreover the anomaly in  $B_{1g}$  softens upon lowering temperature and tends to saturate suggesting a quasi-critical behavior. In Fig. 2(a) we report a comparison between our theoretical calculations and experimental data. According to the neutron-scattering experiments in this material [19, 21] we choose  $\mathbf{q}_c$  along the  $(1,0)$  or  $(0,1)$  directions, giving a non-vanishing vertex for the  $B_{1g}$  symmetry only. We adjust at one temperature the overall intensity by choosing the vertex strength  $\Lambda_{B_{1g}}$  of Eq. (2) and the ultraviolet cutoff  $\omega_0$  to reproduce the lineshape. Then, keeping fixed these parameters at all temperatures, we tune the mass  $m(T)$  to reproduce all the curves. The agreement is manifestly satisfactory, indicating that the strong temperature dependence of the Raman absorption peaks is basically ruled by the temperature dependence of the low-energy scale  $m(T)$  and by

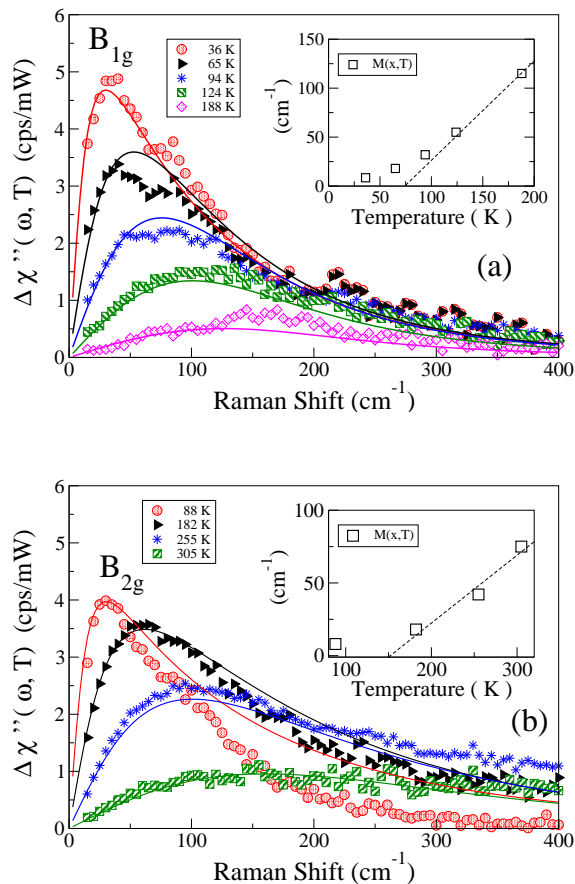


FIG. 2: (color online) (a) Comparison between experimental and calculated Raman spectra on  $\text{La}_{1.90}\text{Sr}_{0.10}\text{CuO}_4$ . The intensity is chosen to reproduce the data with  $\Lambda_{B_{1g}}^2 = 1.7$ , the high-frequency cutoff is  $\omega_0 = 250 \text{ cm}^{-1}$ , and the mass is reported in the inset. (b) Same as (a) for  $\text{La}_{1.98}\text{Sr}_{0.02}\text{CuO}_4$  with  $\Lambda_{B_{2g}}^2 = 0.85$ .

the temperature dependence of the Bose factors. The inset reports the CM mass  $m(x = 0.10, T)$  needed to fit the experimental curves: At large to moderate temperatures  $m(T)$  has a linear part, which has an intercept on the  $T$  axis at a temperature  $T^*$  of the order of  $70 \text{ K}$ . At lower temperatures  $m$  tends to saturate and the system crosses over to a nearly ordered regime with a finite  $m(T)$ . This behavior is clearly consistent with the behavior expected for the mass of critical modes in the underdoped region: At large temperatures the system is in the quantum critical regime with  $m \propto (T - T^*)$ , while below a crossover temperature  $T^*$  [which for LSCO at  $x = 0.10$  is indeed about  $60 - 80 \text{ K}$ , see, e.g., Fig. (1a) of Ref.15] the CO transition is quenched by other effects.

If the CM had wavevectors along the diagonal (1,1) and (1,-1) directions and small modulus, the role of the  $B_{1g}$  and  $B_{2g}$  would be interchanged, with this latter displaying the anomalous Raman absorption. Noticeably, experiments in  $\text{La}_{1.98}\text{Sr}_{0.02}\text{CuO}_4$ , [12], where neutron scattering detect spin incommensurate (but likely also stripe)

order along the diagonal directions [23], do show that the anomalous Raman absorption is present in the  $B_{2g}$  symmetry and is absent in the  $B_{1g}$ . Fig. 2(b) reports a comparison between experimental data of Ref. [12] and a calculated CM contribution for this  $B_{2g}$  case. In this case, consistently with the expected high value of  $T^*$ , the temperature dependence of the mass no longer displays a clear linear behavior and therefore the extrapolation of the high-temperature “linear” part to identify  $T^*$  is not well justified. Nevertheless, as a crude estimate from the last three points we obtain  $T^*$  of the order of  $150 \text{ K}$ , which is again consistent with the  $T^*$  values reported in the literature (see, e.g., Ref. 15). Notice also that the tail of the data at the lowest temperature ( $T = 88 \text{ K}$ ), substantially lower than  $T^*$ , is not well reproduced by our calculations based on a diffusive form of the CM.

A similar behavior of the Raman spectra is observed in  $(\text{Y}_{1.97}\text{Ca}_{0.3})\text{Ba}_2\text{CuO}_{6.05}$  sample [13] at filling  $p = 0.03$ , with a temperature-dependent peak in the  $B_{2g}$  symmetry only. Again it is quite natural to attribute this peak to stripe fluctuations along the  $(1, \pm 1)$  directions and long wavelength [ $\mathbf{q}_c \approx (p, p)$ ]. Fig. 3 reports the comparison between experiments and our theoretical analysis. Again a value of  $T^* \sim 120 \text{ K}$  may be extrapolated from the high temperature mass behavior.

The data for YBCO also display a remarkable change in the lineshape at the lowest temperatures (more pronounced than in  $\text{La}_{1.98}\text{Sr}_{0.02}\text{CuO}_4$  at  $T = 88 \text{ K}$ ). In particular the peak at  $T = 11.0 \text{ K}$  is much narrower and decreases more rapidly at high frequencies. This change in the lineshape naturally marks a change in the nature of the charge fluctuations from the the high-temperature diffusive behavior in the quantum critical regime to a sharper mode behavior typical of the low-temperature underdoped regime. In this case the diffusive form of the propagator fails in reproducing the lineshape, while a good description may be obtained by a factorized form, according to previous treatments of the nearly ordered underdoped regime [24]. Therefore we also carried out the calculations using

$$\tilde{D}(\mathbf{q}, \omega_n) = W(i\omega_n) J_x(\mathbf{q}) J_y(\mathbf{q}), \quad (6)$$

where  $J_{x,y}(\mathbf{q}) = \mathcal{N} \gamma [\gamma^2 + (q_{x,y} - q_{cx,y})^2]^{-1}$ . Here  $\mathcal{N}$  is a normalization factor and the inverse correlation length is  $\gamma$ . The (real-frequency)-dependent part  $W(\omega) = \int d\nu \tilde{A}(\nu) 2\nu / (\omega^2 - \nu^2)$  with  $\tilde{A}(\omega) \sim \Gamma / [(\omega - \omega_{CM})^2 + \Gamma^2]$  is a normalized lorentzian centered around the typical CM energy  $\omega_{CM}$  with halfwidth  $\Gamma$ .  $\Delta\chi_B''$  now reads  $\Delta\chi_B'' = B(T) f(\omega/\Gamma, T/\Gamma, \omega_{CM}/\Gamma)$  with  $B(T) \propto \tilde{g}(T)^4 / [\gamma(T)^2 \Gamma(T)]$ ,  $\tilde{g}$  being the coupling between the CM and the QP [25]. As shown by the dashed curves in Fig. 3, the factorized “propagator” provides a good description at the lowest temperature, while in the intermediate-temperature regime ( $T = 86.2 \text{ K}$ ,  $T = 127.3 \text{ K}$ ) the diffusive propagator becomes progressively a better description of the charge fluctuations. We also notice that

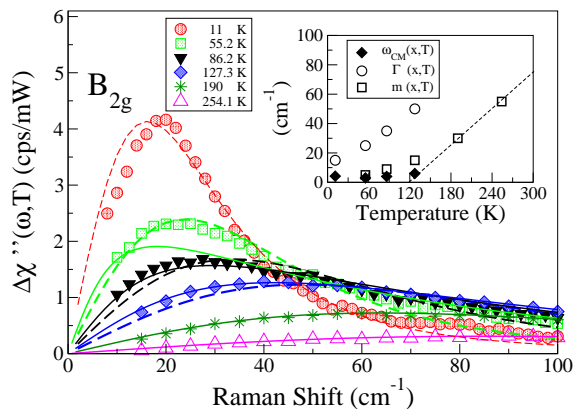


FIG. 3: (Color online) Comparison between experimental and calculated Raman spectra on  $(Y_{1.97}Ca_{0.3})Ba_2CuO_{6.05}$  with diffusive propagators [Eq. (1)] (solid lines). The intensity is chosen to fit the data with  $\Lambda_{B_{2g}}^2 = 0.41$ , the high-frequency cutoff is  $\omega_0 = 100 \text{ cm}^{-1}$ , and the mass is reported in the inset. The dashed lines are obtained with factorized “propagators” [Eq. (6)] with overall intensity  $B(T) = 28, 27, 19, 12$  (cps/mW) for  $T = 11 \text{ K}, 55.2 \text{ K}, 86.2 \text{ K}, 127.3 \text{ K}$ .  $\Gamma(T)$  and  $\omega_{CM}$  are also reported in the inset.

the mass  $m(T)$  of the quantum-critical diffusive propagator smoothly connects with the energy of the low-temperature modes:  $m(T) \sim \omega_{CM}$ .

As far as LSCO samples are concerned, the diffusive form of the modes seems to persist down to the lowest temperatures in the available published data. We notice in passing that the two values for  $T^*$  obtained at  $x = 0.02$  and  $x = 0.10$  linearly extrapolate to  $T^* = 0$  at  $x = x_c \approx 0.17$ , consistent with the theoretical position of the CO quantum critical point [8, 15] and not inconsistent with most of the experiments on  $T^*$  in LSCO [11].

In order to emerge clearly from the other electronic excitations, the CM’s need to have rather small masses (from the insets of Figs. 2 and 3 a few tens of  $\text{cm}^{-1}$ ). This is the case in underdoped systems where the finite and sizable values of  $T^*$  carry to finite temperature the small values of the mass, which should vanish at  $T_{CO}(x) \sim T^*$  if a genuine long-range order would occur. Around optimal doping, where  $T_{CO}(x_c) = 0$ , anomalous peaks are hardly visible because superconductivity intervenes at higher temperatures before the mass, being proportional to  $T$ , becomes sufficiently small. Similarly we argue that the observation of CM peaks in Bi-2212 systems is unlikely. In these materials, STM experiments suggest that the CO coherence length is smaller than 5-6 lattice spacings [20], indicating large mass values, in contrast to underdoped LSCO materials, where according to neutron scattering experiments the stripe correlations may extend over tens of lattice spacings [19].

In summary we calculated the CO-CM contribution to the Raman response function. The idea that charge modes are important in the low-energy Raman spectra

is also supported by recent experiments in ladder compounds [26]. Here we showed that the CM contribution quantitatively accounts for the observed anomalous peaks in Raman spectra of LSCO and YBCO. In this explanation a crucial role is played by the symmetry of the Raman vertices: We demonstrate the stringent connection between the symmetry properties of the Raman spectra and the doping, which implies a dependence of the CM on *finite* wavevectors specific of stripe or eggbox fluctuations as inferred from neutron scattering. This rules out for the interpretation of these Raman experiments local (*i.e.*, at all momenta) excitations like polarons, disorder-localized single particles or resonating-valence-bond singlets. Also spin CM do not comply with these symmetry requirements over the whole doping range examined above. For the same reason other excitations peaked at  $\mathbf{q} = 0$  (like superconducting pair fluctuations or time-reversal-breaking current fluctuations) are not appropriate. Although we cannot *a priori* exclude that the proposed CO collective excitations are concomitant with these other more elusive forms of criticality, at the moment the anomalous Raman absorption can only be interpreted with CM peaked at finite momenta.

We acknowledge interesting discussions with C. Castellani, T. Devereaux, and J. Lorenzana. We particularly thank R. Hackl and L. Tassini for discussions and for providing us the Raman data before publication. We acknowledge financial support from the MIUR-COFIN2003 n. 2003020230\_006. C.D.C. thanks the Walther Meissner Institute in Garching and the Humboldt Foundation for hospitality and support.

- 
- [1] A. Lucarelli *et al.*, Phys. Rev. Lett. **90**, 037002 (2003).
  - [2] M. Dumm, *et al.*, Phys. Rev. Lett. **88**, 147003 (2002).
  - [3] S. Lupi, *et al.*, Phys. Rev. B **62**, 12418 (2000).
  - [4] E. J. Singley, *et al.*, Phys. Rev. B **64**, 224503 (2001).
  - [5] S. Caprara, C. Di Castro, S. Fratini, and M. Grilli, Phys. Rev. Lett. **88**, 147001 (2002).
  - [6] Ar. Abanov, A. Chubukov, and J. Schmalian, Adv. Phys. **52**, 119 (2003) and references therein.
  - [7] C. M. Varma, Phys. Rev. Lett. **75**, 898 (1995); Phys. Rev. B **55**, 14554 (1997) and references therein.
  - [8] C. Castellani, C. Di Castro, and M. Grilli, Phys. Rev. Lett. **75** 4650 (1995).
  - [9] W. Metzner, D. Rohe, and S. Andergassen, Phys. Rev. Lett. **91**, 066402 (2003) and references therein.
  - [10] M. Capone, M. Fabrizio, C. Castellani, and E. Tosatti, Phys. Rev. Lett. **93**, 047001 (2004).
  - [11] J.L. Tallon, J.W. Loram, Physica C **349**, 53 (2001); C. Castellani, C. Di Castro, and M. Grilli, J. of Phys. and Chem. of Sol. **59**, 1694 (1998).
  - [12] L. Tassini *et al.*, cond-mat/0406169 (unpublished).
  - [13] R. Hackl and L. Tassini, private communication.
  - [14] See, e.g., T. P. Devereaux, A. Virosztek, and A. Zawadowski, Phys. Rev. B **51**, 505 (1995).
  - [15] S. Andergassen, S. Caprara, C. Di Castro, and M. Grilli,

- Phys. Rev. Lett. **87**, 056401 (2001).
- [16] L. G. Aslamazov and A. I. Larkin, Sov. Phys. Sol. State **10**, 875 (1968).
- [17] B. R. Patton and L. J. Sham, Phys. Rev. Lett. **31**, 631 (1973); *ibid.* **33**, 638 (1974).
- [18] S. Takada and E. Sakai, Prog. Th. Phys. **59**, 1802 (1978).
- [19] J. M. Tranquada, *et al.*, **375**, 561 (1995).
- [20] C. Howald, *et al.*, Phys. Rev. B **67**, 014533 (2003); M. Vershihin, *et al.*, Science **303**, 1995 (2004).
- [21] K. Yamada, *et al.*, Phys. Rev. B **57**, 6165 (1998).
- [22] F. Venturini, *et al.*, Phys. Rev. B **66**, 060502(R) (2002).
- [23] S. Wakimoto, *et al.*, Phys. Rev. B **60**, R769 (1999).
- [24] A. P. Kampf and J. R. Schrieffer, Phys. Rev. B **42**, 7967 (1990).
- [25] The intensity of the spectra  $B(T)$  has a temperature dependence through  $\gamma(T)$ ,  $\Gamma(T)$ , and  $\tilde{g}(T)$ . This latter in the “factorized-propagator” scheme is proportional to the (local) order parameter [24]. These dependencies saturate at low T and lead to an increasing and saturating  $B(T)$  for  $T$  much smaller than  $T^*$ .
- [26] A. Gozar, *et al.*, Phys. Rev. Lett. **91**, 087401 (2003).